

Supporting Information For

Construction of heterostructured NiFe₂O₄-C nanorods by transition metals recycling from the simulated electroplating sludge leaching solution for high performance lithium ion batteries

Xueqian Lei,^{†,#} Youpeng Li,^{†,#} Changzhou Weng,[†] Yanzhen Liu,[†] Weizhen Liu,^{*,†}
Junhua Hu,[§] Zhang Lin,[†] Chenghao, Yang,^{*,†} Meilin Liu[‡]

[†]*School of Environment and Energy, South China University of Technology, Guangzhou 510006, P. R. China*

[§]*School of Materials Science and Engineering, Zhengzhou University, Zhengzhou, 450001, China*

[‡]*School of Materials Science and Engineering Georgia Institute of Technology, Atlanta, GA 30332-0245, USA*

*Corresponding author, *E-mail*: weizhliu@scut.edu.cn (W. Liu); esyangc@scut.edu.cn (C. Yang)

X. Lei and Y. Li contributed equally to this work.

Figures and Tables

Table S1. Content analysis of metals in raw electroplating sludge and acid-leaching solution by ICP.

Elements	Ni	Fe	Cu	Zn	Al	Si	Na	Ca	Mg
Content in electroplating sludge (mg/kg)	170861	135698	19378	22739	16658	35680	13848	26480	7725
Percentage content (%)	17.09	13.57	1.94	2.27	1.67	3.57	1.39	2.65	0.77
Concentration in acid-leaching solution (mg/L)	28132.8	22163.4	882.5	956.2	832.3	554.8	2682.4	3187.5	1099.8
Extraction efficiency (%)	82.33	81.66	22.77	21.03	24.98	7.77	96.85	60.19	71.18

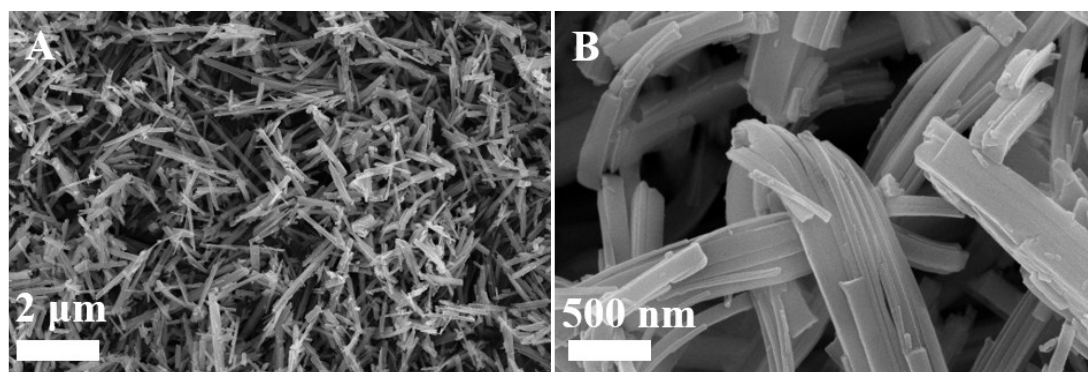


Fig. S1 SEM images of Fe-Ni-C precursors with different magnifications.

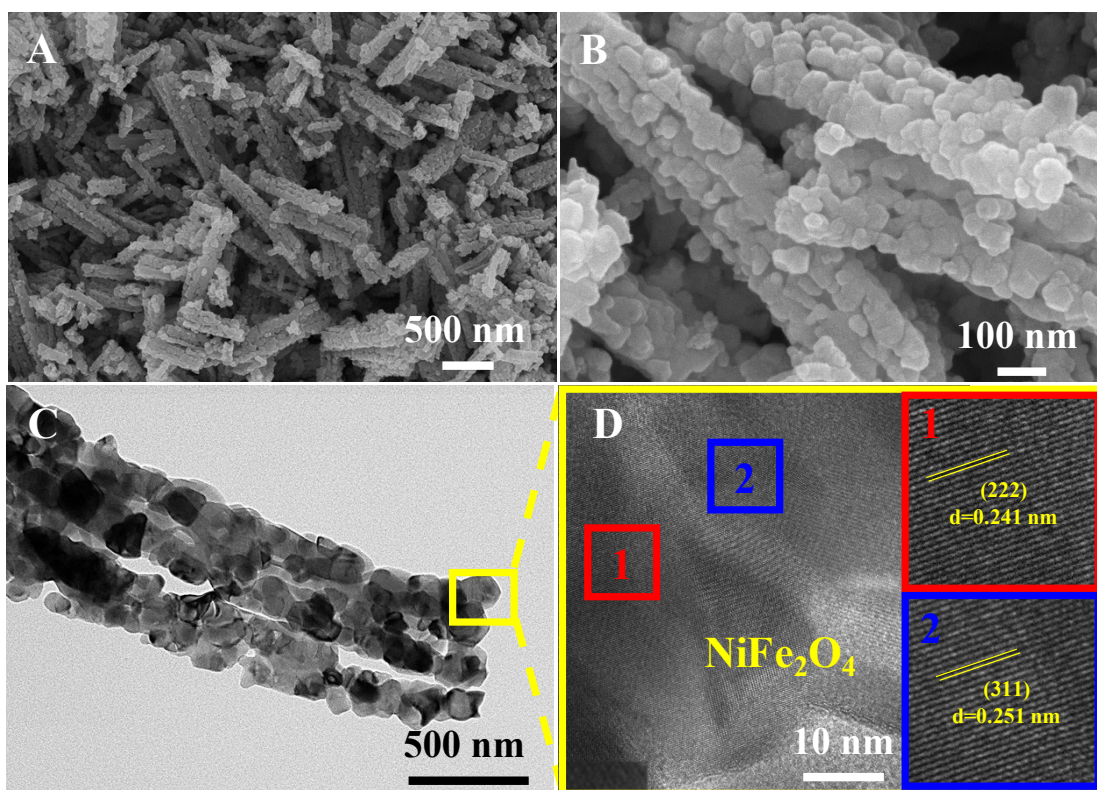


Fig. S2 (A&B) SEM, (C) TEM and (D) HRTEM images of NiFe₂O₄ nanorods.

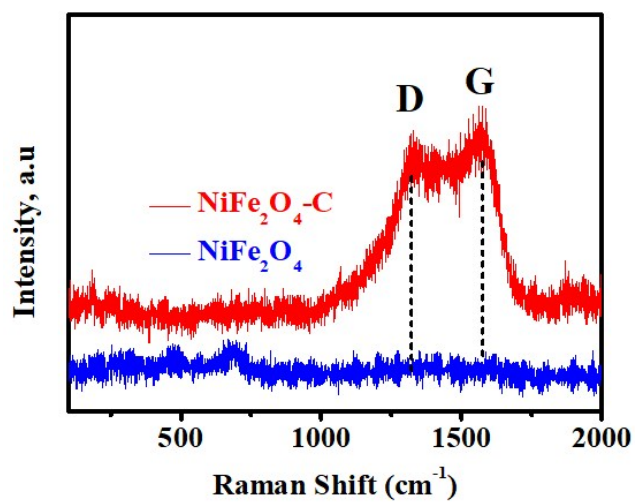


Fig. S3 Raman spectra of the NiFe₂O₄ and NiFe₂O₄-C nanorods.

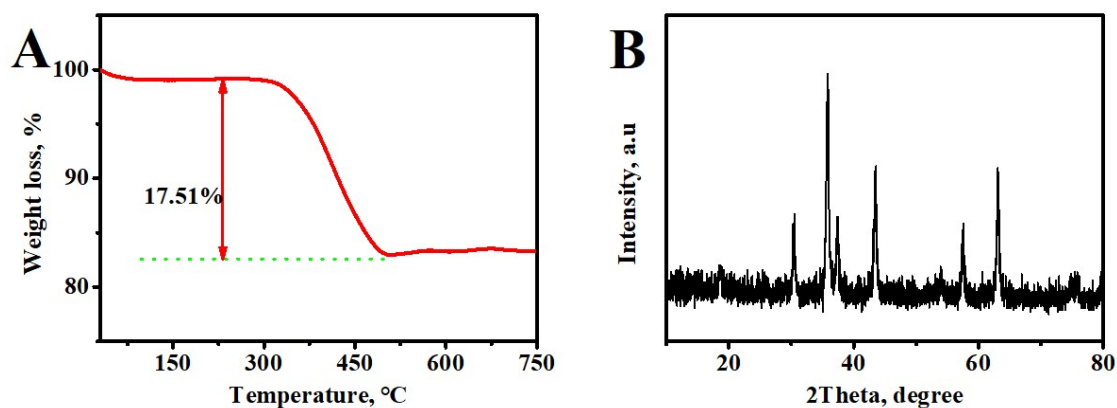


Fig. S4 (A) TGA curve of NiFe₂O₄-C nanorods and (B) XRD pattern of the final products after TGA testing.

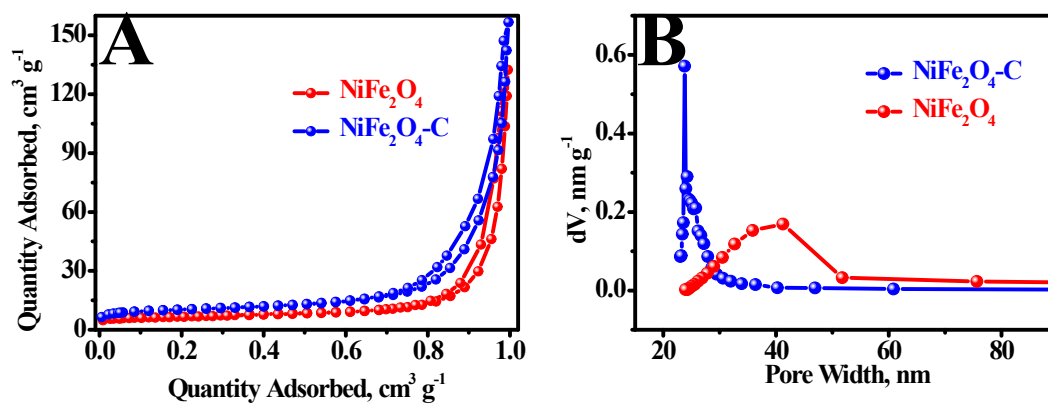


Fig. S5 (A) N₂ adsorption/desorption isotherms and (B) pore size distribution of NiFe₂O₄-C and NiFe₂O₄ nanorods.

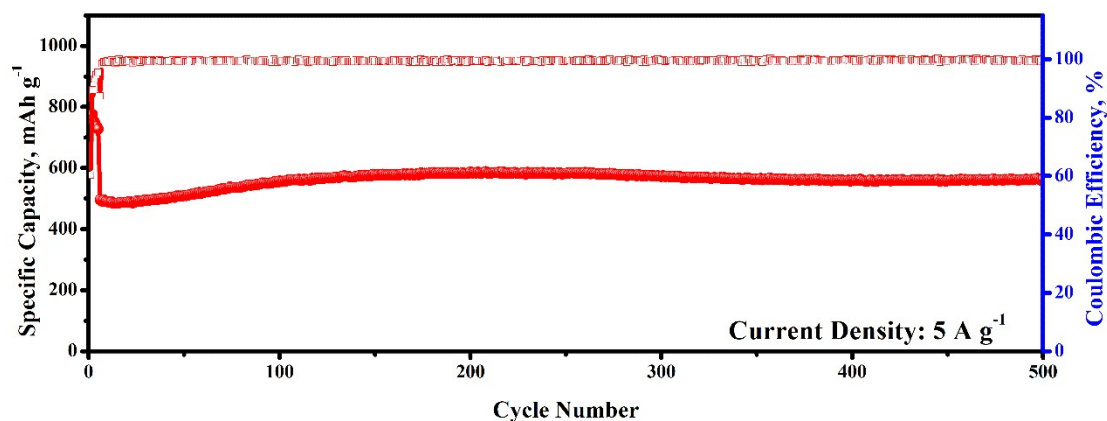


Fig. S6 Long-term cycling performance of NiFe₂O₄-C nanorods at 5 A g⁻¹.

Table S2 The electrochemical performance comparison of NiFe₂O₄-C nanorods fabricated in this work with other reported anode materials in LIBs.

Types of materials	Cycling performance		Rate performance		Ref.
	Capacity	Current	Capacity	Current	
	(mAh g ⁻¹)/cycles	(A g ⁻¹)	(mAh g ⁻¹)	(A g ⁻¹)	
NiFe ₂ O ₄ /C hollow spheres	1266/100	0.2	1195	0.2	[S1]
NiFe ₂ O ₄ /rGO nanoplatelets	1105/50	0.1	1031	0.4	[S2]
NiFe ₂ O ₄ /MWCNTs nanohybrid	871/25	0.2	958	0.2	[S3]
Porous NiFe ₂ O ₄ /Si microspheres	906/100	0.1	677	0.2	[S4]
LiPON coated NiFe ₂ O ₄ thin film	849/50	5μA cm ⁻²	840	5μA cm ⁻²	[S5]
Fe ₃ O ₄ / NiFe ₂ O ₄ nanosheets	500/750	0.2	1437	0.2	[S6]
NiFe ₂ O ₄ /EG nanocomposites	601/800	1	667	0.2	[S7]
NiFe ₂ O ₄ spherical nanoparticles	786/100	0.5	1057	0.2	[S8]
NiFe ₂ O ₄ porous nanorods/graphene composites	655/600	1	1053	0.2	[S9]
NiFe ₂ O ₄ @NC nano octahedrons	1297/50	0.1	630	2	[S10]
NiFe ₂ O ₄ @C fibers	497/100	0.1	390	0.2	[S11]
ultrathin NiO/ NiFe ₂ O ₄ nanoplates	200/25	0.1	400	0.1	[S12]
NiFe₂O₄-C nanorod	972.3/200	0.1	502.1	5	This work

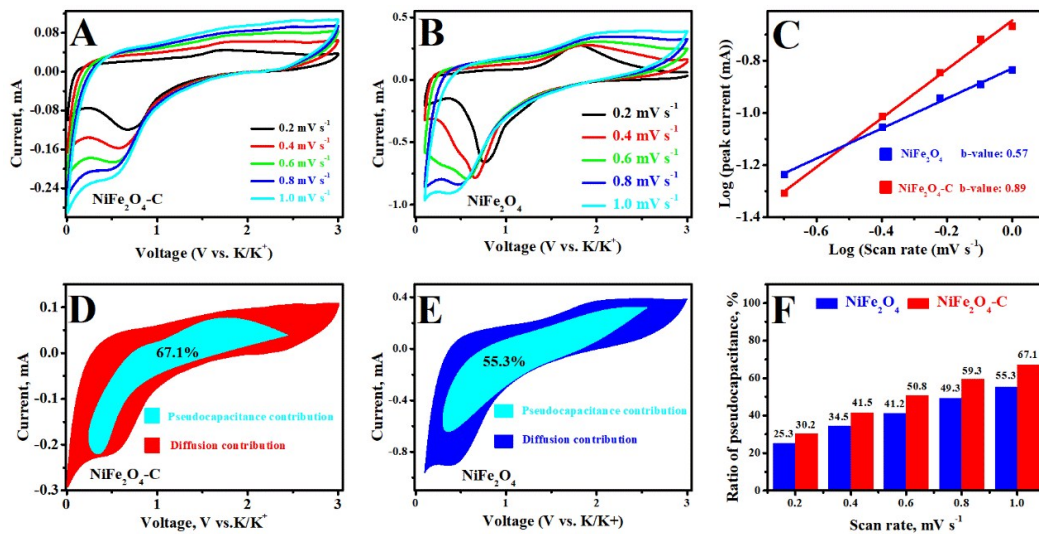


Fig. S7 CV curves at different scan rate for NiFe₂O₄-C (A) and NiFe₂O₄ (B); b-value

for NiFe₂O₄-C and NiFe₂O₄ (C); Contribution of the surface-driven process at 1 mV s⁻¹ in NiFe₂O₄-C (D) and NiFe₂O₄ (E); Capacitance contribution of NiFe₂O₄-C and NiFe₂O₄ at different scan rates.

Generally, the Li⁺ storage behavior in transition metal oxides endows greatly ratio of pseudocapacitance contribution. Thus, the pseudocapacitance contribution process of NiFe₂O₄-C and pure NiFe₂O₄ are investigated quantitatively. The cyclic voltammetry (CV) curve for both NiFe₂O₄-C and pure NiFe₂O₄ with different scan rate (0.2-1.0 mV s⁻¹) at the voltage window of 0.1-3.0 V are firstly collected in Fig. S7A and B. According to the previous reported, the equation between the peak current (*i*) and scan rate (*v*) can be summarized as the following relationship:^{S13}

$$i = av^b$$

The *b*-value could be ensured by the slope of Log(*i*) versus Log(*v*). If the value of *b* is approximate to 0.5, the Li⁺ storage behavior is mainly determined by the diffusion controlled process. As contrast, the reaction process between the Li⁺ and NiFe₂O₄ is primly related to the pseudocapacitance behavior when the *b*-value is much closer to 1.^{S14} In this work, the *b*-value for both NiFe₂O₄-C and pure NiFe₂O₄ are 0.93 and 0.81 (Fig. S7C), respectively, which confirmed that their Li⁺ storage process are two step course consisting of diffusion-driven process and pseudocapacitance contribution, and the NiFe₂O₄-C have a higher ratio of pseudocapacitance contribution compared with that of pure NiFe₂O₄. Hence, the value of pseudocapacitance contribution ratio could be calculated by the following equation:^{S15}

$$i = k_1v + k_2v^{1/2}$$

where the i is the actual current, v is the scan rate, the k_1 and k_2 is constants, the k_1v and $k_2v^{1/2}$ represent the surface capacitive and diffusion controlled course. The pseudocapacitance contribution ratio for both $\text{NiFe}_2\text{O}_4\text{-C}$ and NiFe_2O_4 exhibit a gradual upward trend along with the increase of scan rate, and the $\text{NiFe}_2\text{O}_4\text{-C}$ shows a higher ratio compared with that of NiFe_2O_4 (Fig. S7F). Based on the Dunn's method, the distribution diagram ratio of surface-controlled process is 67.1%, confirming that the enhanced electrochemical performance is related to the pseudocapacitance process (Fig. S7D, E).

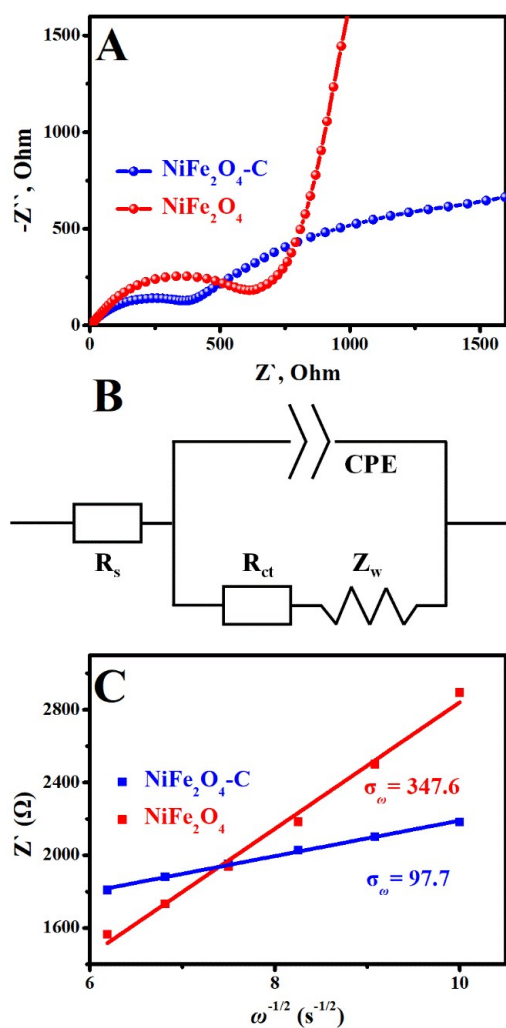


Fig. S8 (A) EIS spectra, (B) corresponding equivalent circuit model, and (C) the relationship of Z' versus $\omega^{-1/2}$ at low frequency region of NiFe_2O_4 and $\text{NiFe}_2\text{O}_4\text{-C}$.

Table S3 The simulated results from electrochemical impedance spectra of NiFe₂O₄ and NiFe₂O₄-C samples.

Sample	R_s (Ω)	R_{ct} (Ω)	D_{Li^+} ($\text{cm}^{-2} \text{s}^{-1}$)
NiFe ₂ O ₄	6.1	549.9	0.92×10^{-14}
NiFe ₂ O ₄ -C	4.8	321.1	3.28×10^{-14}

The Li⁺ ions diffusion coefficient (D_{Li^+}) of NiFe₂O₄-C and NiFe₂O₄ can be calculated according to the following equation:^{S16}

$$D_{Li^+} = R^2 T^2 / 2 A^2 n^4 F^4 C^2 \sigma_w \omega^{-1/2}$$

where R is the gas constant, T is the absolute temperature, A is the surface area of the cathode, n is the number of electrons per molecule during oxidization, F is the Faraday constant, C is the concentration of Li⁺ ion, σ_w is the Warburg factor which is calculated by the following equation:^{S17}

$$Z' = R_s + R_{ct} + \sigma_w \omega^{-1/2}$$

R_s is the resistance of the electrolyte and electrode material, R_{ct} is the charge transfer resistance and ω is the angular frequency in the low frequency region.

References

- S1 R. Jin, H. Jiang, Y. Sun, Y. Ma, H. Li and G. Chen, *Chem. Eng. J.*, 2016, **303**, 501.
- S2 C. Li, X. Wang, S. Li, Q. Li, J. Xu, X. Liu, C. Liu, Y. Xu, J. Liu, H. Li, P. Guo and X.S. Zhao, *Appl. Surf. Sci.*, 2017, **416**, 308.
- S3 M. Mujahid, R. U. Khan, M. Mumtaz, S. A. Soomro and S. Ullah, *Ceram. Int.*, 2019, **45**, 8486.
- S4 Q. Liang, W. Zhou, X. Hou, C. Wei, H. Qin and F. Chen, *Mater. Lett.*, 2019, **238**, 70.
- S5 K. Wei, Y. Zhao, Y. Cui, J. Wang, Y. Cui, R. Zhu, Q. Zhuang and M. Xue, *J. Alloy. Compd.*, 2018, **769**, 110.
- S6 H. Xu, X. Wang, H. Liu, J. Wang, X. Dong, G. Liu, W. Yu, Y. Yang and H. Zhang, *J. Mater. Sci.*, 2018, **53**, 15631.
- S7 Y. Xiao, J. Zai, B. Tian and X. Qian, *Nano-Micro Lett*, 2017, **9**, 34.
- S8 M. Islam, G. Ali, M. Jeong, W. Choi, K.Y. Chung and H. Jung, *ACS Appl. Mater. Inter.*, 2017, **9**, 14833.
- S9 M. Fu, Z. Qiu, W. Chen, Y. Lin, H. Xin, B. Yang, H. Fan, C. Zhu and J. Xu, *Electrochim. Acta.*, 2017, **248**, 292.
- S10 X. Liu, T. Zhang, Y. Qu, G. Tian, H. Yue, D. Zhang and S. Feng, *Electrochim. Acta.*, 2017, **231**, 27.
- S11 T. Dong, G. Wang and P. Yang, *Diam. Relat. Mater.*, 2017, **73**, 210.
- S12 D. Du, W. Yue, X. Fan, K. Tang and X. Yang, *Electrochim. Acta.*, 2016, **194**, 17.
- S13 X. Ma, X. Xiong, P. Zou, W. Liu, F. Wang, L. Liang, Y. Liu, C. Yuan and Z. Lin,

Small., 2019, **15**, 1903259.

S14 Y. Li, C. Yang, F. Zheng, X. Ou, Q. Pan, Y. Liu and G. Wang, *J. Mater. Chem. A.*, 2018, **6**, 17959.

S15 Y. Li, W. Zhong, C. Yang, F. Zheng, Q. Pan, Y. Liu, G. Wang, X. Xiong and M. Liu, *Chem. Eng. J.*, 2019, **358**, 1147.

S16 C. Yang, X. Liang, X. Ou, Q. Zhang, H. S. Zheng, F. Zheng, J. H. Wang, K. Huang and M. Liu, *Adv. Funct. Mater.*, 2019, **19**, 1807971.

S17 Y. Li, C. Yang, F. Zheng, Q. Pan, Y. Liu, G. Wang, T. Liu, J. Hu and M. Liu, *Nano. Energy.*, 2019, **59**, 582.